

Large Scale Anisotropic Bias from Primordial non-Gaussianity

Shant Baghrām,^{1,*} Mohammad Hossein Namjoo,^{2,†} and Hassan Firouzjahi^{1,‡}

¹*School of Astronomy, Institute for Research in Fundamental Sciences (IPM), P. O. Box 19395-5531, Tehran, Iran*

²*School of Physics, Institute for Research in Fundamental Sciences (IPM), P. O. Box 19395-5531, Tehran, Iran*

In this work we study the large scale structure bias in models of anisotropic inflation. We use the Peak Background Splitting method in Excursion Set Theory to find the scale-dependent bias. We show that the amplitude of the bias is modified by a direction-dependent factor. In the specific anisotropic inflation model which we study, the scale-dependent bias vanishes at leading order when the long wavelength mode in squeezed limit is aligned with the anisotropic direction in the sky. We also extend the scale-dependent bias formulation to the general situations with primordial anisotropy. We find some selection rules indicating that some specific parts of a generic anisotropic bispectrum is picked up by the bias parameter. We argue that the anisotropic bias is mainly sourced by the angle between the anisotropic direction and the long wavelength mode in the squeezed limit.

I. INTRODUCTION

Inflation [1] has emerged as the leading paradigm for the theory of early universe and structure of formation. Basic predictions of inflation indicate that the curvature perturbations are nearly scale-invariant, nearly adiabatic and nearly Gaussian which are in very good agreements with cosmological observations such as WMAP [2]. The simplest models of inflation are based on a scalar field rolling slowly on a flat potential. On the other hand, the observations from Planck satellite are expected to improve the constraints on primordial non-Gaussianity(PNG) significantly. Any detection of primordial non-Gaussianity will have significant implications for inflationary model buildings, for a review see [3–5]. For example, many models of single field inflation predict a very small amount of local non-Gaussianity in the squeezed limit [6] $f_{NL} \sim (n_s - 1)$ in which n_s is the curvature perturbation power spectrum spectral index and f_{NL} parametrizes the amplitude of local non-Gaussianity(NG). With $n_s \simeq 0.97$ from WMAP [2], one expects $f_{NL} < 1$ for conventional models of single field inflation. However, this expectation is violated if the system is not reached the attractor regime [7, 8] or if one allows for a non Bunch-Davies initial condition [9–11]. Furthermore, inflationary models with large non-Gaussianity predicts different shapes for bispectrum. Therefore, any detection or otherwise of large primordial non-Gaussianity with different shapes will go a long way to rule out many inflationary scenarios or put constraints on model parameters.

The most suitable cosmological observation to constrain the primordial non-Gaussianity is CMB. This is because the perturbations in the last scattering surface are in the linear regime and the fingerprints of non-Gaussianity are mainly preserved [12, 13]. However, recently the interests in LSS observations and their implications for non-Gaussianity are boosted due the theoretical findings of scale-dependent bias [14]. In general, the distribution of baryonic matter in the Universe, mainly clustered in galaxies and the clusters of galaxies, is the fundamental observable of LSS [15, 16]. The distribution of galaxies and clusters of galaxies can be studied by a): Probability distribution function (PDF) of structures (mass function of structures), and b): The correlation functions, power spectrum and even higher moments of distribution.

In the standard theories of structure formation, the Gaussianity assumption plays a crucial role in finding the distribution of structures via the primordial density contrast distribution [17]. Accordingly, changing the initial condition from a Gaussian to non-Gaussian primordial density perturbations will change the PDF of structures. This change mainly shows itself in the tail of distribution function. Consequently, this effect manifests itself mainly in the statistics of the clusters of galaxies in high mass and high redshifts distributions [18–22].

The emergence of non-Gaussianity will introduce a non-zero bispectrum in LSS observations, however the gravitational instabilities are also the source of higher order nonzero moments [23]. The gravitational instability has its own signatures on the bispectrum of structures, but its shape changes in deep non-linear regime. So the bispectrum of galaxies and clusters of galaxies is not a very efficient observational tool to detect the primordial non-Gaussianity.

*Electronic address: baghrām-AT-ipm.ir

†Electronic address: mh.namjoo-AT-ipm.ir

‡Electronic address: firouz-AT-ipm.ir

However, the primordial non-Gaussianity changes the background linear density fluctuations, which in turn it also influences the density peaks where structures are formed. The effect of background density fluctuations, affecting the halo abundance of dark matter, is known as bias parameter. The non-Gaussianity has a very unique feature in LSS by introducing a scale-dependent bias [14, 24]. This special fingerprint of primordial non-Gaussianity provides the opportunity to constrain primordial non-Gaussianity using the power spectrum of galaxies. Also there are other LSS observables such as the Integrated Sachs Wolfe cross correlation with the galaxy power spectrum [25], the 3D bispectrum of Ly-alpha forest and the redshifted 21-cm signal from the post re-ionization epoch [26, 27], the statistics of voids [28] etc. which can also be used to study the primordial non-Gaussianity. In a word, the LSS observations will become very important tools, complementary to CMB observations, to constrain the properties of primordial non-Gaussianity.

There have been some indications of statistical anisotropies on CMB power spectrum. Although The statistical significance of the violation of statistical isotropy is not high [29, 30], but nonetheless the possibility of having statistically anisotropic seed perturbations are intriguing. The statistical anisotropy is usually parameterized via [31] $\mathcal{P}_\zeta = \mathcal{P}_{\zeta_0}(1 + g_*(\hat{k} \cdot \hat{n})^2)$ in which \hat{n} is the preferred direction in sky, \mathcal{P}_ζ is the curvature perturbation power spectrum of the Fourier mode \vec{k} with the direction along the unit vector \hat{k} and \mathcal{P}_{ζ_0} represents the isotropic power spectrum. Constraints from CMB and large scale structure indicate that $|g_*| \lesssim 0.4$ [32, 33]. Recently the bispectrum and the trispectrum in a model of anisotropic inflation [34] have been calculated in [35–38]. It has been shown that large non-Gaussianities with non-trivial shapes are generated. Considering our motivation in using non-Gaussianity fingerprints in LSS as a probe of inflationary universe, we would like to study the effects of large scale-dependent and orientation-dependent bispectrum on bias in these models.

The rest of the paper is organized as follows. In Section II we present the anisotropic inflation model and the corresponding bispectrum which is used in subsequent analysis. In Section III we review the basics of halo bias with non-Gaussian initial conditions. In Section IV we present our results of halo bias in the models of anisotropic inflation with the anisotropic bispectrum obtained in Section II. In Section V, we present a general mathematical formulation for the anisotropic bispectrum in terms of spherical harmonics which can be used to calculate the halo bias in models with generic anisotropic bispectrum. We leave some technical issues of halo bias analysis into appendix.

II. ANISOTROPIC INFLATIONARY MODEL

In this section we review the anisotropic inflation model and its anisotropic bispectrum which will be used in subsequent analysis.

The best method to introduce statistical anisotropies is to incorporate $U(1)$ gauge fields or vector fields in models of inflation. However, due to conformal invariance of the standard Maxwell theory in an expanding background, the background gauge field and its quantum fluctuations are diluted during inflation. Therefore, in order to produce an almost scale-invariant power spectrum of gauge field fluctuations, one has to consider a time-dependent gauge kinetic coupling. This prescription was originally used in [39, 40] in the context of primordial magnetic field. An interesting model of anisotropic inflation is introduced in [34] in which it is shown that, with a suitably chosen gauge kinetic coupling, the inflationary system has an attractor solution in which the gauge field energy density reaches a small but observationally detectable fraction of the total energy density. As a result, the anisotropy produced are at the order of slow-roll parameters.

The Lagrangian of the system is

$$S = \int d^4x \sqrt{-g} \left[\frac{M_P^2}{2} R - \frac{1}{2} \partial_\mu \phi \partial^\mu \phi - \frac{f^2(\phi)}{4} F_{\mu\nu} F^{\mu\nu} - V(\phi) \right], \quad (1)$$

in which ϕ is the inflaton field and $F_{\mu\nu} = \partial_\mu A_\nu - \partial_\nu A_\mu$ is the field strength associated with the $U(1)$ gauge field A_μ .

The background is in the form of Bianchi I universe with the metric

$$\begin{aligned} ds^2 &= -dt^2 + e^{2\alpha(t)} \left(e^{-4\sigma(t)} dx^2 + e^{2\sigma(t)} (dy^2 + dz^2) \right) \\ &= -dt^2 + a(t)^2 dx^2 + b(t)^2 (dy^2 + dz^2). \end{aligned} \quad (2)$$

Here $H \equiv \dot{\alpha}$ is interpreted as the average Hubble expansion rate, $H_a \equiv \dot{a}/a$ and $H_b \equiv \dot{b}/b$ are the expansion rates along the spatial directions x and y and $\dot{\sigma}/H \equiv (H_b - H_a)/H$ is a measure of anisotropic expansion. We note that this metric enjoys only a two-dimensional rotational symmetry in $y - z$ plane.

The details of the dynamics of the system are given in [34, 37]. For the simple chaotic potential $V = m^2 \phi^2/2$, the conformal coupling (the time-dependent gauge kinetic coupling) is chosen to be

$$f(\phi) = \exp\left(\frac{c\phi^2}{2M_P^2}\right), \quad (3)$$

with c a constant. With $c \simeq 1$, one can check that the system admits the attractor solution in which the ratio of the gauge field energy density in the form of electric field energy density is a small and constant fraction of the total energy density. Defining the fraction of electric field energy density to the potential energy as

$$R \equiv \frac{\dot{A}^2 f(\phi)^2 e^{-2\alpha}}{2V}, \quad (4)$$

during the attractor regime one obtains

$$R = \frac{c-1}{2c} \epsilon_H = \frac{I}{2} \epsilon_H, \quad (5)$$

in which $\epsilon_H \equiv -\dot{H}/H^2$ is the slow-roll parameter and $I \equiv \frac{c-1}{c}$.

The power spectrum of the curvature perturbation,

$$\langle \zeta_{\mathbf{k}} \zeta_{\mathbf{k}'} \rangle = (2\pi)^3 P_\zeta(\mathbf{k}) \delta^3(\mathbf{k} + \mathbf{k}') \quad , \quad \mathcal{P}_\zeta \equiv \frac{k^3}{2\pi^2} P_\zeta(\mathbf{k}), \quad (6)$$

for the particular anisotropic inflation described above was calculated in [35–38, 41–46] which has the form

$$P_\zeta(\vec{k}) = P_0 \left(1 + g_* (\hat{k} \cdot \hat{n})^2\right), \quad (7)$$

where the anisotropy parameter g_* is given by

$$g_* \equiv -24IN(k_1)N(k_2). \quad (8)$$

Here $N(k_i)$ represents the number of e-folding that the mode of interest k leaves the horizon. In our notation, the number of e-folding is counted backwards from the time of end of inflation by $a(N) = a_f \exp(N)$ so $N \leq 0$. For example, $N = N_{CMB} = -60$ to solve the flatness and the horizon problem. As a result, $N(k)$ is calculated to be

$$N(k) - N_{CMB} = \ln\left(\frac{k}{k_{CMB}}\right), \quad (9)$$

in which k_{CMB} represents the comoving mode which leaves the horizon at $N_{CMB} = -60$ e-folds before the end of inflation. To satisfy the observational constraints from CMB and large scale structure $|g_*| < 0.3$, we require $I \lesssim 10^{-5}$.

The bispectrum of curvature perturbations, $B_\zeta(\vec{k}_1, \vec{k}_2, \vec{k}_3)$, is defined via

$$\langle \zeta(\vec{k}_1) \zeta(\vec{k}_2) \zeta(\vec{k}_3) \rangle \equiv (2\pi)^3 \delta^3(\vec{k}_1 + \vec{k}_2 + \vec{k}_3) B_\zeta(\vec{k}_1, \vec{k}_2, \vec{k}_3). \quad (10)$$

The Bispectrum for the model of anisotropic inflation was calculated using in-in formalism in [35, 36] and using δN formalism in [37] with the result

$$B_\zeta(\vec{k}_1, \vec{k}_2, \vec{k}_3) = 288IN(k_1)N(k_2)N(k_3) \left(C(\vec{k}_1, \vec{k}_2) P_0(k_1) P_0(k_2) + 2\text{perm.} \right). \quad (11)$$

Here the anisotropic shape function $C(\vec{k}_1, \vec{k}_2)$ is defined as:

$$C(\vec{k}_1, \vec{k}_2) \equiv \left(1 - (\hat{k}_1 \cdot \hat{n})^2 - (\hat{k}_2 \cdot \hat{n})^2 + (\hat{k}_1 \cdot \hat{n})(\hat{k}_2 \cdot \hat{n})(\hat{k}_1 \cdot \hat{k}_2) \right), \quad (12)$$

where \hat{n} is the specific anisotropic direction in the sky. Note that in Eq. (11), $P_0(k_i)$ represents the isotropic power spectrum so all anisotropies are encoded in shape function $C(\vec{k}_1, \vec{k}_2)$ (and the appropriate permutations) with the amplitude $288IN(k_1)N(k_2)N(k_3)$.

It is instructive to look into the bispectrum in the squeezed limit in which one mode is much longer than the other two, say $k_3 \ll k_1 \simeq k_2$, so from the condition $\sum_i \vec{k}_i = 0$ we also conclude that $\vec{k}_1 \simeq -\vec{k}_2$. In this limit, one obtains

$$B_\zeta(k_1, k_2, k_3) \simeq 24P_0(k_1)P_0(k_3)|g_*(k_1)|N(k_3) \times \left[1 - (\hat{k}_1 \cdot \hat{n})^2 - (\hat{k}_3 \cdot \hat{n})^2 + (\hat{k}_1 \cdot \hat{n})(\hat{k}_3 \cdot \hat{n})(\hat{k}_1 \cdot \hat{k}_3)\right] \quad (k_3 \ll k_1 \simeq k_2) \quad (13)$$

in which to obtain the above result, Eq. (8) have been used to express the parameter $IN(k_1)N(k_2)$ in terms of g_* .

The non-Gaussianity parameter f_{NL} is defined in the squeezed limit $k_3 \ll k_1 \simeq k_2$ via

$$f_{NL}(\vec{k}_1, \vec{k}_2, \vec{k}_3) = \lim_{k_3 \rightarrow 0} \frac{5}{12} \frac{B_\zeta(\vec{k}_1, \vec{k}_2, \vec{k}_3)}{P_\zeta(k_1)P_\zeta(k_3)}. \quad (14)$$

In general, f_{NL} is an orientation-dependent and scale-dependent quantity. As an order of magnitude estimation, and neglecting the logarithmic scale-dependence in $N(k_i)$, we can define an orientation-dependent effective f_{NL}^{eff} via

$$f_{NL}^{eff} = 240IN_{CMB}^3(k_1)C(\vec{k}_1, \vec{k}_2), \quad (15)$$

where $N(k) = N_{CMB} + \ln(k/k_{CMB})$. Setting $N_{CMB} = 60$, we can easily get $f_{NL}^{eff} \sim 60$ with $g_* \sim 0.1$, compatible with observational constraints.

A very interesting observation from Eq.(13) is that when the long wavelength mode \vec{k}_3 is in the direction of anisotropy, i.e. $\vec{k}_3 \parallel \hat{n}$, then the term inside the big-bracket in Eq.(13) vanishes. Consequently, in this configuration, we do not expect to see the non-Gaussian effects in LSS. We discuss this feature in more details in Sec.III

For the subsequent analysis we adopt the coordinate system such that the anisotropic direction \hat{n} coincides with the \hat{z} direction in the spherical coordinates so the other momentum vectors are described by $\hat{k}_1 = (\theta_1, \psi_1)$ and $\hat{k}_2 = (\theta_2, \psi_2)$, where θ and ψ are the polar and azimuthal angles in spherical coordinates, respectively. For the future reference, we also need the angles between two arbitrary unit vectors $\hat{q}_i = (\theta_{q_i}, \psi_{q_i})$ defined via $\cos \gamma = \hat{q}_1 \cdot \hat{q}_2$, which is

$$\cos \gamma = \sin(\theta_{q_1}) \sin(\theta_{q_2}) \cos(\psi_{q_1} - \psi_{q_2}) + \cos \theta_{q_1} \cos \theta_{q_2}. \quad (16)$$

The power spectrum and the bi-spectrum presented in Eqs. (7) and (11) are for the particular model of anisotropic inflation as studied in [35–37]. For a generic anisotropic model the most general power spectrum can be written as [47]

$$P(\vec{k}) = P_0(k) \left[1 + \sum_{LM} g_{LM}(k) Y_{LM}(\hat{k}) \right], \quad (17)$$

where P_0 is the isotropic power spectrum, $Y_{LM}(\hat{k})$ (with $L \geq 2$) are spherical harmonics and $g_{LM}(k)$ quantify the departure from statistical isotropy as a function of wavenumber k . As each Fourier mode \vec{k} is related to $-\vec{k}$, in the case of real $g_{LM}(k)$, the multipole moment L must be even, and in the limit of $k \rightarrow 0$ we will recover the isotropic power spectrum $P_0(k)$. However, in the general case, (real and imaginary g_{LM}), we have:

$$g_{LM}^* = (-1)^L g_{L-M}. \quad (18)$$

This condition is imposed by the fact that the matter power spectrum is a real quantity.

Comparing Eq. (17) with Eq. (7) for our particular anisotropic inflation model we have $g_{20} \propto g_*$ while the rest of g_{LM} are zero. In Section V we extend the general definition of Eq. (17) for the power spectrum to the bispectrum and look into its implications in halo bias analysis.

III. BIAS

In this section we review the concept of the bias, a parameter that shows the dependence of dark matter halo abundance to the background dark matter density perturbations. The reader who is familiar with these analysis can directly jump to next Section in which we present our results of halo bias for anisotropic inflation model. It is worth to mention that in this work we are not interested in galaxy bias, which is the weighted integral of the halo bias, corresponding to the mechanism of the halo occupation distribution (HOD).

We follow the work by Scoccimarro et al. [48], to find an expression for the bias. The halo bias relates the halo abundance to the dark matter overdensity, in Excursion Set Theory (EST), (also known as Extended Press Schechter (EPS))[49], defined by:

$$b(k, z) = \frac{\delta_h}{\delta_m}, \quad (19)$$

where δ_h is the halo overdensity and δ_m is the matter density perturbation. The EST framework is very useful as it provides a non-perturbative model (that includes e.g. exclusion effects at small scales) [50]. At large scales EST is known to reproduce the Gaussian initial condition while in small scales it determines the local bias parameter with linear and nonlinear terms [51, 52] which are in reasonably good agreements with numerical simulations [53–55].

It is worth to mention that the halo bias is a function of redshift and scale. This scale-dependance is introduced by applying the initial Non-Gaussian condition. Bias parameter in the context of peak-background splitting (PBS) [56, 57] is described by the fact that the background large scale overdensity changes the critical threshold of spherical collapse [58] such that the collapse criteria will be :

$$\delta_s > \delta_c - \delta_l, \quad (20)$$

where δ_s is the matter density contrast of the structure, (the subscript "s" stands for short wavelength); δ_l is the background (long-wavelength) density contrast and $\delta_c \simeq 1.68$ is the critical density contrast in spherical collapse formalism.

Now in order to find the bias parameter we have to compare the dark matter halo abundance, in cases with and without the presence of long wavelength (background) overdensity. For this task we use the Excursion Set theory approach. In the Appendix A, we review the concept of EPS in more details and we will derive the bias parameter using the PBS in EPS context. For a review of PBS see Appendix A.

According to Appendix A the large scale halo biasing can be treated in peak-background splitting [56]. The idea of splitting of the density contrast to short and long wavelength can be translated to a similar splitting of Bardeen potential due to Poisson equation, which depends on cosmological parameters. The matter density in PBS can be written as:

$$\rho = \bar{\rho}(1 + \delta_s + \delta_l). \quad (21)$$

The number density of formed structures with mass m can be expressed as a function of small scale statistics, (i.e. small scale power spectrum $P_s(k)$) and the background long wave-length perturbation δ_l (i.e. $n = n[\delta_l(\vec{x}), P_s(k_s); m]$) [59].

The primordial potential in Fourier space can be translated to the late time potential as:

$$\Phi(k, z) = \Phi_{ini} \times T(k)D(z)(1 + z), \quad (22)$$

Where Φ_{ini} is the initial Bardeen potential sourced by the inflation field quantum fluctuations, $T(k)$ is the transfer function and $D(z)$ is the growth function normalized to scale factor at early times. Now due to Poisson equation one can relate the initial non-Gaussian potential to δ_l via Poisson equation in sub-horizon scale and linear-regime:

$$\delta_l = M(k, z)\Phi, \quad (23)$$

where

$$M(k, z) = \frac{2k^2 T(k)D(z)}{3\Omega_m^0 H_0^2}. \quad (24)$$

Here, Ω_0 and H_0 are the matter fraction energy density and Hubble parameter at present time, respectively.

In order to calculate the halo-bias term, we should calculate the effect of large scale perturbation, δ_l , on the probability distribution function(PDF) of structures. This yields the following relation between the Lagrangian halo number density and PDFs [48]

$$1 + \delta_h^L = \frac{\partial_m \int_{\infty}^{\delta_c} \Pi(\delta_s, \sigma_m^2, \delta_c; \delta_l, \sigma_l^2) d\delta_s}{\partial_m \int_{\infty}^{\delta_c} \Pi_0(\delta_s, \sigma_m^2, \delta_c) d\delta_s} \quad (25)$$

where, $\Pi(\delta_s, \sigma_m^2, \delta_c; \delta_l, \sigma_l^2)$ is the conditional PDF, which means that the variance σ_m at large scales converges to the value $\sigma_m = \sigma_l$, in contrast with unconditional PDF, $\Pi_0(\delta_s, \sigma_m^2, \delta_c)$, in which the variance vanishes ($\sigma_m \rightarrow 0$) at large scales.

It will be relevant to define a quantity that shows the probability of first up-crossing in the time interval between σ_m^2 and $\sigma_m^2 + d\sigma_m^2$, in EST language as:

$$\mathcal{F}_0(\delta_c, \sigma_m^2) \equiv -\frac{\partial}{\partial \sigma_m^2} \int_{-\infty}^{\delta_c} \Pi_0(\delta_s, \sigma_m^2, \delta_c) d\delta_s, \quad (26)$$

From the above formalism, we can see the effect of primordial NG on LSS. Assuming that the Bardeen Potential has a local-type non-Gaussianity we have

$$\Phi = \phi + f_{NL}\phi^2 \quad (27)$$

where ϕ is the Gaussian field. Now we can use the splitting idea on ϕ by applying $\phi = \phi_l + \phi_s$, where ϕ_l is long wavelength mode of potential and ϕ_s is short wavelength corresponding to the scale of structure. In Appendix A we discuss how the above non-linear form can be generalized to a model with arbitrary shape of non-Gaussianity, in which case, the non-linear term generalizes to a kernel.

Now in the presence of primordial non-Gaussianity, the modes are not independent and the conditional PDF is modified by the non-Gaussian long-wavelength mode. In this case the PDF will be a function of ϕ_l through the variance and also higher order cumulants ($c_p \equiv \langle \delta_s^p \rangle_c$) as:

$$\Pi(\delta_s, \sigma_m^2, \delta_c; \delta_l, 0) \rightarrow \Pi[\delta_s, \sigma^2(\phi), c_p(\phi), \delta_c; \delta_l(\phi), 0], \quad (28)$$

That is, unlike the case of Gaussian initial condition that only the variance depends on the long-wavelength, in the case of non-Gaussianity the higher cumulants are also affected. Under the assumption that all these effects are small, and also using the Markovian random walk in EST formalism we can Taylor expand the conditional PDF, Π , around unconditional one, Π_0 . For details, see appendix A.

In this work we study the linear bias effect of anisotropic primordial non-Gaussianity and include only the first derivative contribution in Taylor expansion, Eq.(A15). As we show in appendix A, up to first order in f_{NL} , only the first two terms in Taylor expansion of PDF appear. These terms are derivatives of PDF with respect to the long wavelength mode δ_l and the variance σ_l . The higher order terms corresponding to derivatives with respect to c_p ($p \geq 3$) contribute to $\mathcal{O}(f_{NL}^2)$ and $\mathcal{O}(g_{NL})$ bias.

As we mentioned, in this work we only study the first order effect in f_{NL} . The $p = 1$ contribution, the first term in Taylor expansion, Eq.(A16), is the usual scale-independent linear bias from Gaussian perturbations. Keeping in mind $b \equiv \delta_h/\delta_l$, for the first order linear bias (b_{1L}) we have

$$p = 1 : \quad b_{1L} = \frac{\partial_m \int (\partial \Pi / \partial \delta_l)_0}{\partial_m \int \Pi_0} = \left[\frac{\partial}{\partial \delta_l} \ln \left(\frac{dn(\delta_l)}{d \ln m} \right) \right], \quad (29)$$

which can be written as:

$$b_{1L} = \frac{\partial}{\partial \delta_l} \ln(n(\delta_l)). \quad (30)$$

In the presence of primordial non-Gaussianity, there are new contributions from higher order cumulants $p \geq 2$. As a result, the next to leading order term, gives

$$p = 2 : \quad b_{2L} = \frac{\partial_m [I_{21} \int \partial \Pi_0 / \partial \sigma_m^2]}{M(k) \partial_m \int \Pi_0}, \quad (31)$$

which in general is a scale-dependent correction to the leading order, scale-independent bias (A18). The key quantity here is I_{21} which is the derivative of second cumulant σ_m^2 , ($p = 2$), with respect to the long wavelength mode ϕ_l which is obtained as [48]:

$$I_{21}(k, m) = \frac{1}{P_\phi(k)} \int B_{\hat{\delta}\hat{\delta}\phi}(q, k-q, -k) d^3q, \quad (32)$$

where $B_{\hat{\delta}\hat{\delta}\phi}$ is the cross bispectrum of small-scale smoothed density $\hat{\delta}$ and ϕ . As a result, I_{21} is the quantity which we are looking for in the case of non-Gaussian initial condition which introduces scale-dependent bias of the order of $\mathcal{O}(f_{NL})$.

So far only the Lagrangian bias appeared because peaks are those of the initial density field (linearly extrapolated). Making the standard assumptions that halos move coherently with the underlying dark matter, and using the techniques outlined in [60–63], one can obtain the final Eulerian bias as:

$$b_E = 1 + b_{1L} + b_{2L}; \quad (33)$$

Now Assuming the Markovian behavior of density fields and universality of mass function we will have:

$$b_{1L} = \frac{2}{\delta_c} \partial_{\ln \sigma_m^2} \ln(\sigma_m^2 \mathcal{F}) = b_{1L(G)} + b_{1L(NG)}, \quad (34)$$

A very important point is that in above equation we omit the subscript of \mathcal{F} , which means that the non-Gaussianity will change the PDF of structures, so the first linear term will have a contribution from primordial non-Gaussianity. Consequently, we have:

$$b_{1L(G)} = \frac{2}{\delta_c} \partial_{\ln \sigma_m^2} \ln(\sigma_m^2 \mathcal{F}_0) \quad (35)$$

and

$$b_{1L(NG)} = \frac{2}{\delta_c} \partial_{\ln \sigma_m^2} \ln(\sigma_m^2 \mathcal{R}_{NG}) = \frac{\partial \ln \mathcal{R}_{NG}(m, f_{NL})}{\partial \delta_l}, \quad (36)$$

where $\mathcal{F} = \mathcal{R}_{NG} \mathcal{F}_0$, and \mathcal{R}_{NG} comes from the deviation of PDF from the Gaussian case [21, 64]. In other words, the effects of non-Gaussianity appeared both in the PDF and the power spectrum via scale-dependent bias parameter. Since in this work we are interested in the scale-dependence features of bias, the contribution of \mathcal{R}_{NG} is not much of interest. For the Gaussian case we use the Sheth and Tormen [65] Gaussian mass function. For the non-Gaussian PDF effect we use the results of [18] in which they used the idea of expanding the non-Gaussian PDF in the Press-Schechter framework [17] in which \mathcal{R}_{NG} is defined as:

$$\mathcal{R}_{NG}(m, f_{NL}) = 1 + \frac{1}{6} x(x^2 - 3) s_3(x) - \frac{1}{6} (x - 1/x) \frac{ds_3(x)}{d \ln(x)}, \quad (37)$$

where $x \equiv \delta_c / \sigma_M$ and $\delta_c = 1.68$ is the critical density and s_3 is the reduced skewness defined as:

$$s_3(R) \equiv \frac{\langle \delta_R^3 \rangle}{\langle \delta_R^2 \rangle^{3/2}} = \frac{\langle \delta_R^3 \rangle}{\sigma_m^3}, \quad (38)$$

The skewness is related to the matter bispectrum as:

$$\langle \delta_R^3 \rangle = \int \frac{d^3 q_1}{(2\pi)^3} \frac{d^3 q_2}{(2\pi)^3} W(Rq_1) W(Rq_2) W(Rq_{12}) M(q_1, z) M(q_2, z) M(q_{12}, z) B_0(q_1, q_2, q_{12}), \quad (39)$$

where $q_{12} = q_1 + q_2$, W is the window function in Fourier space and R is the smoothing scale. For more detail see Appendix A.

On the other hand, the scale-dependent bias can be rewritten by

$$b_{2L} = \frac{I_{21}(k, m)}{2\sigma_m^2 M(k, z)} \delta_c b_{1L} + \frac{1}{M(k, z)} \partial_{\ln \sigma_m^2} \left(\frac{I_{21}(k, m)}{\sigma_m^2} \right) \quad (40)$$

So the total Eulerian bias up to first order in f_{NL} can be split into the scale-independent b_{si} and scale-dependent b_{sd} terms as:

$$b_{t(E)} = b_{si} + b_{sd} \quad (41)$$

where b_{si} and b_{sd} are:

$$b_{si} \equiv b_G + b_{1L(NG)}, \quad (42)$$

with $b_G \equiv 1 + b_{1L(G)}$ and

$$b_{sd} = b_{2L} + \mathcal{O}(f_{NL}^2) + \mathcal{O}(g_{NL}) + \dots \quad (43)$$

In the next section we find the scale-independent and scale-dependent bias and discuss the effect of the primordial anisotropy in the bias parameter.

IV. ANISOTROPIC BIAS

In this section we study the LSS bias in the model of anisotropic inflation. For a related work with a phenomenological modeling of bispectrum and its implication for bias see [66].

In this work we assume that the mechanism of spherical collapse for structure formation is still applicable in our model with primordial anisotropic perturbations. This is motivated from the fact that the collapse mechanism is a local process so up to first order it is not affected by large scale anisotropies. Secondly, we assume that the transfer function at leading order is not affected by the anisotropic terms in energy-momentum tensor of cosmic fluid. It would be interesting to perform the analysis with the above assumptions are relaxed but this is beyond the scope of this work.

For this task we investigate the change in PDF and corresponding cumulants, and the effect of these changes on bias. First of all the variance is defined through the linear matter power spectrum:

$$\sigma^2(M, z) = \int \frac{d^3k}{(2\pi)^3} P_L(k) W^2(kR), \quad (44)$$

where P_L and $W(kR)$ are linear matter power spectrum and window function in Fourier space which are discussed the details in Appendix A.

In our model the variance is modified due to the fact that we use anisotropic power spectrum. However, we show below that it is not direction-dependent. Without loss of generality, we can assume that the anisotropy is pointed along the z -direction in spherical coordinates ($\hat{n} = \hat{z}$). Then, starting from Eq. (7) for the primordial anisotropic power spectrum, we have

$$\sigma_A^2(m, z) = \int d\psi d\cos\theta dk k^2 P_0(k, z) [1 + g_*(k) \cos^2\theta] W(kR) \simeq (1 + \frac{g_*}{3}) \sigma_m^2 \quad (45)$$

where θ and ψ are spherical coordinate angles and $g_*(k) = -24IN(k_1)N(k_2)$. Note that σ_A^2 is the variance obtained from the full anisotropic power spectrum whereas σ_m^2 is the variance corresponding to the isotropic part. Since the scale-dependence of g_* is logarithmic through $N(k_i)$, as given in Eq. (9), we can ignore its scale-dependence as a first approximation, so we have the last approximate equality in Eq.(45). Note that, as we mentioned before, the variance does not have any direction-dependence, which is somewhat an obvious observation, since one should integrate over the full 3D Fourier space to obtain the variance, eliminating any direction present in power spectrum. However, it is interesting to note that the correction to the variance due to anisotropy enhances or suppresses the leading order term, depending on the sign of anisotropy parameter g_* . From the above variance, we can obtain the leading order scale-independent bias b_{1L} .

As for the next step, we obtain the bias from the anisotropic bispectrum which is both scale-dependent and direction-dependent. This would be the main effect of anisotropy in the bias parameter. In order to obtain b_{2L} , we need I_{21} where the information from primordial bispectrum is encoded. We use the squeezed limit ($k_3 \ll k_2 \simeq k_1$) bispectrum predicted by the model, Eq.(13). Because of symmetry in $x - y$ plane we rotate the long wavelength mode such that $\psi_{\hat{k}_3} = 0$. Inserting the bispectrum to I_{21} , Eq.(32) results in

$$I_{21}(\mathbf{k}, z, m) = 24 \int d\psi_q d(\cos\theta_q) dq q^2 M_m(q, z) M_m(|k - q|, z) P_\phi(q) N(k) |g_*(q)| \times [1 - \cos^2\theta_q - \cos^2\theta_k + \cos\theta_q \cos\theta_k (\sin\theta_q \sin\theta_k \cos\psi_q + \cos\theta_q \cos\theta_k)] \quad (46)$$

where k and q correspond to long and short wavelength (k_3 and k_2 in Eq. (13)), and θ, ψ are polar and azimuthal angles in spherical coordinates, defined by the angle between the anisotropy direction \hat{n} and wavenumbers \hat{q} and \hat{k} respectively:

$$\cos\gamma_q = \hat{q} \cdot \hat{n} = \sin\theta_{\hat{n}} \sin\theta_{\hat{q}} \cos(\psi_{\hat{n}} - \psi_{\hat{q}}) + \cos\theta_{\hat{n}} \cos\theta_{\hat{q}}, \quad (47)$$

$$\cos\gamma_k = \hat{k} \cdot \hat{n} = \sin\theta_{\hat{n}} \sin\theta_{\hat{k}} \cos(\psi_{\hat{n}} - \psi_{\hat{k}}) + \cos\theta_{\hat{n}} \cos\theta_{\hat{k}}, \quad (48)$$

Now we can integrate the angular dependence γ_q which yields

$$I_{21}(k, z, m, \theta_k) = 64\pi N(k) (1 - \cos^2\theta_k) \int dq q^2 M_{m,z}(q) M_{m,z}(|k - q|) P_\phi(q) |g_*(q)|. \quad (49)$$

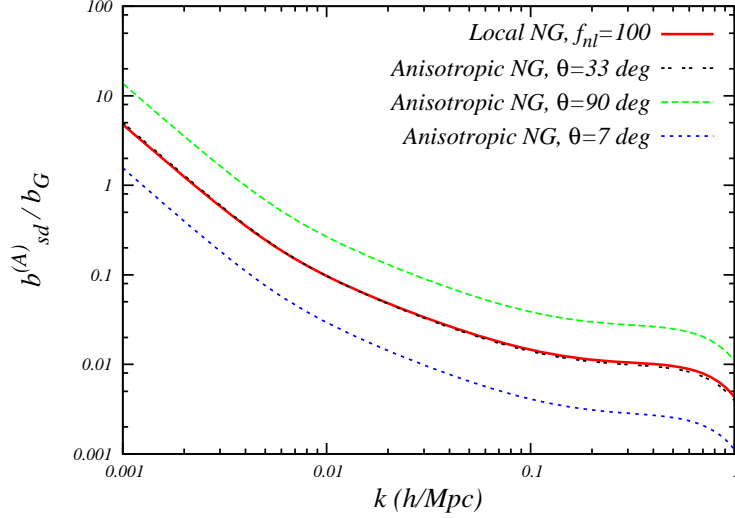


FIG. 1: The fraction of Scale dependent anisotropic bias Eq.(55), to the Gaussian bias, $b_{sd}^{(A)}/b_G$, is plotted versus the wavenumber for different angles between the long wavelength mode and the anisotropy direction. The black double-dashed curve, the green long-dashed curve and the blue dotted curve, respectively, are for $\theta_k = 33^\circ$, $\theta_k = 90^\circ$ and $\theta_k = 7^\circ$. The solid red line indicates the local non-Gaussianity with $f_{NL} = 100$. For the anisotropic bias, we choose $I \simeq 1.9 \times 10^{-6}$ such that $f_{NL}^{eff} = 100$ from Eq. (15). The redshift is $z = 0$.

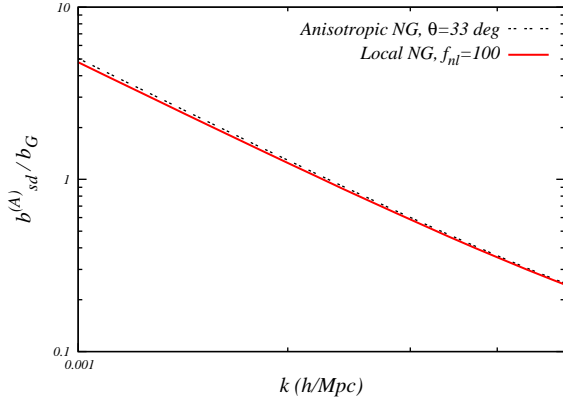


FIG. 2: This figure is a zoom-in of Fig. 1 for long wavelength modes where we compare $b_{sd}^{(A)}/b_G$ of our model with $\theta_k = 33^\circ$ and the local non-Gaussianity with $f_{NL} = 100$. This shows small deviation between the two models due to a mild scale-dependence of g_* parameter.

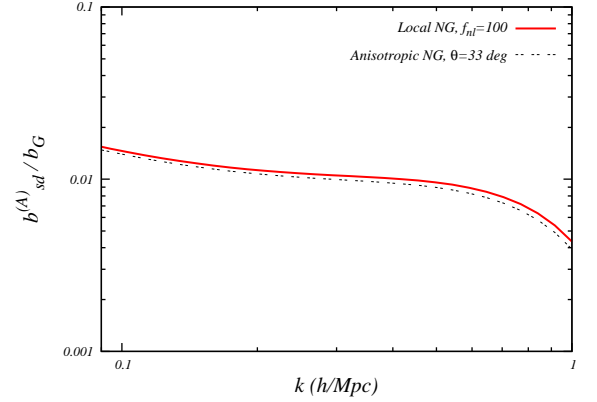


FIG. 3: This figure is a zoom-in of Fig. 1 for short wavelength modes where again we compare $b_{sd}^{(A)}/b_G$ of our model for $\theta_k = 33^\circ$ with the local non-Gaussianity with $f_{NL} = 100$.

It is interesting to note that the orientation-dependence appears in the form of $\sin^2 \theta_k$. As a result, the bias vanishes when $\sin \theta_k = 0$, i.e. when the long wavelength mode is aligned with the anisotropic direction. This result originates from the fact that in this specific direction the bispectrum vanishes in squeezed limit as one can check from Eq. (13). Furthermore, since in the model under consideration g_* has a mild scale-dependence via logarithmic correction in $N(k)$, we observe that there is an extra, but mild k -dependent, factor in I_{21} in comparison with the standard local non-Gaussian shape [48, 67]. Besides that, I_{21} linearly depends on I which is the free parameter of the anisotropic inflationary model. Now, by using the variance and I_{21} parameter obtained above we can find the bias parameter in the anisotropic model by

$$b_{1L} = \frac{\partial_m \int (\partial \Pi / \partial \delta_l)_0}{\partial_m \int \Pi_0} = \left[\frac{\partial}{\partial \delta_l} \ln \left(\frac{dn(\delta_l)}{d \ln m} \right) \right] = b_{1L(G)} + b_{1L(NG)}, \quad (50)$$

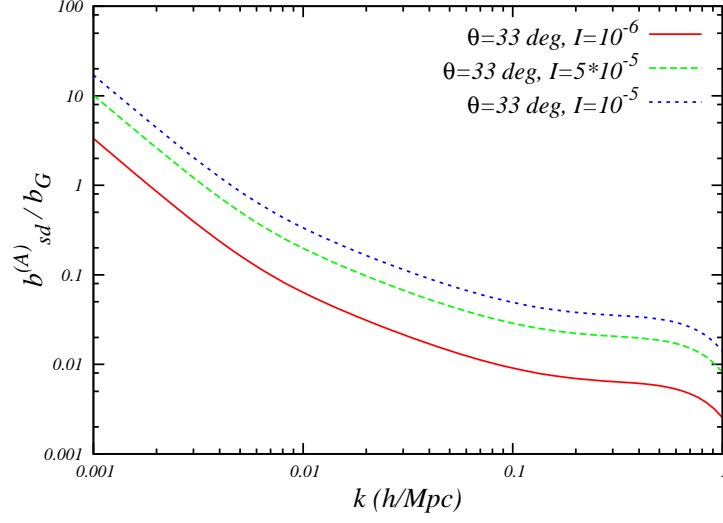


FIG. 4: $b_{sd}^{(A)}/b_G$ is plotted versus wavenumber with $\theta_k = 33^\circ$ for three different values of I . The solid red curve, the green dashed curve and blue dotted curve, respectively, are for $I = 10^{-6}$, $I = 5 \times 10^{-6}$ and $I = 10^{-5}$. In all case we set the redshift $z=0$.

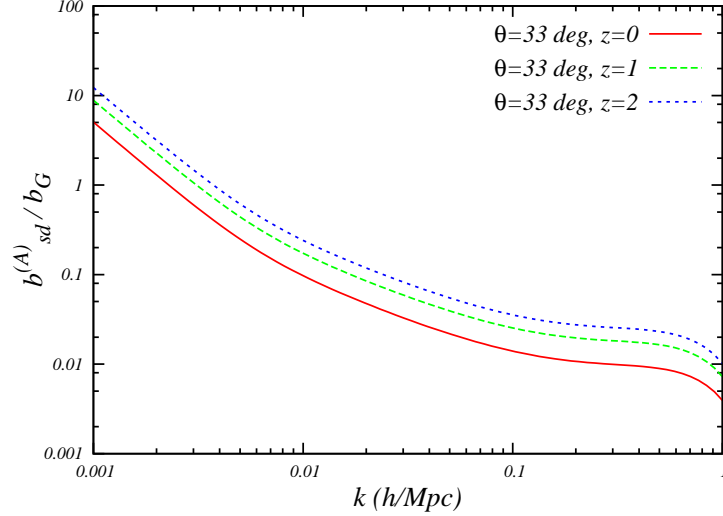


FIG. 5: $b_{sd}^{(A)}/b_G$ is plotted versus wavenumber with $I = 10^{-6}$ and $\theta_k = 33^\circ$ for three different redshifts. The solid red curve, the green dashed curve and the dotted blue curve, respectively, are for $z = 0$, $z = 1$ and $z = 2$.

where, for the first order linear bias in the case of anisotropy, we have

$$b_{(A)1L(NG)} = \frac{2}{\delta_c} \partial_{\ln \sigma_A^2} \ln(\sigma_A^2 \mathcal{R}_{(A)NG}) = \frac{\partial \ln \mathcal{R}_{(A)NG}(m, f_{NL})}{\partial \delta_l}, \quad (51)$$

in which the subscript (A) has been added to point out that the parameters are obtained in the presence of anisotropy. Here $\mathcal{R}_{(A)NG}$ is the anisotropic non-Gaussian correction to the PDF of primordial fluctuations defined by:

$$\mathcal{R}_{(A)NG}(m, f_{NL}) = 1 + \frac{1}{6} x_A (x_A^2 - 3) s_{(A)3}(x_A) - \frac{1}{6} (x_A - 1/x_A) \frac{ds_3(x_A)}{d \ln(x_A)}, \quad (52)$$

where $x_A \equiv \delta_c/\sigma_A$ and $\delta_c = 1.68$ is the critical density and $s_{(A)3}$ is the reduced skewness defined as:

$$s_{(A)3}(R) \equiv \frac{\langle \delta_R^3 \rangle}{\langle \delta_{(A)R}^2 \rangle^{3/2}} = \frac{\langle \delta_{(A)R}^3 \rangle}{\sigma_A^3}. \quad (53)$$

Note that, in the above formula, we have to use the full variance σ_A including the correction due to anisotropy. The anisotropic skewness is also defined as:

$$\langle \delta_{(A)R}^3 \rangle = \int \frac{d^3 q_1}{(2\pi)^3} \frac{d^3 q_2}{(2\pi)^3} W(Rq_1) W(Rq_2) W(Rq_{12}) M(q_1, z) M(q_2, z) M(q_{12}, z) B_A(q_1, q_2, q_{12}), \quad (54)$$

where B_A is the anisotropic bispectrum.

The next order term in bias will give the scale-dependent and direction-dependent effect:

$$b_{sd}^{(A)} = b_{(A)2L}(k, z, m, \theta_k) = \frac{I_{21}(k, z, m, \theta)}{2\sigma_A(m, z)^2 M(k, z)} \delta_c b_{1L} + \frac{1}{M(k, z)} \partial_{\ln \sigma_A^2} \left(\frac{I_{21}(k, m, \theta_k)}{\sigma_A^2(m, z)} \right) \quad (55)$$

So the total Eulerian anisotropic bias is defined as:

$$b_{t(E)} = 1 + b_{1L(G)} + b_{(A)1L(NG)} + b_{(A)2L}, \quad (56)$$

The first three terms above give the scale-independent bias, whereas the last term is scale-dependent and direction-dependent bias due to the anisotropic bispectrum. Since the model we consider has a bispectrum shape very close to the standard local non-Gaussian shape and since $b_{1L(NG)}$ is small in comparison with b_{sd} in local shape, [67], we can ignore $b_{1L(NG)}$ term in our analysis.

In Fig. 1 we plot the relative magnitude of the scale-dependent bias Eq.(55) to Gaussian bias, $b_{(sd)}^{(A)}/b_G$, versus the wavenumber. As expected we have approximately k^{-2} scale-dependence similar to the local non-Gaussian shape. However, this k -dependence is slightly different because of mild dependence of g_* to wavenumber. A completely new feature is the direction-dependence of bias originated from primordial anisotropy, proportional to $\sin^2 \theta_{k_3}$. In the case of $\theta_{k_3} = \pi/2$ we have the maximum scale-dependent bias, whereas at angles $\theta_{k_3} = 0, \pi$, as the anisotropic bispectrum vanishes, the scale-dependent bias also vanishes accordingly.

In order to compare our results with the conventional local non-Gaussian models, we set $\theta_{k_3} = 33^\circ$ to have $f_{NL}^{eff} \simeq 100$ and then compare the bias in this specific direction with the bias in local shape with amplitude $f_{NL} = 100$. In Fig. 2 and Fig. 3, for both long and short wavelengths, we compare the fraction of scale-dependent bias, $b_{(sd)}/b_G$, from local non-Gaussianity with our anisotropic model. Since $g_* \propto N(k) = N_{CMB} + \ln(k/k_{CMB})$, for long wavelength modes the bias of our model is slightly higher than local non-Gaussian case while it is slightly lower for short wavelength modes.

The free parameter of our model is I . In Fig. 4 we plot $b_{(sd)}^{(A)}/b_G$ versus wave number for different values of I . The I -dependence of bias is linear according to Eq. (49). In Fig. 5 we investigate the redshift-dependence of $b_{(sd)}^{(A)}/b_G$. At higher redshifts we have higher bias. This is the standard expectation, since at earlier times the non-linearity of local, small scale perturbations were weaker and thus they are more sensitive to large scale perturbations, resulting in larger bias.

V. GENERAL FORMULATION

In this section we calculate the bias, assuming a general model independent primordial anisotropy. For this task we write the power spectrum and bispectrum in their most general anisotropic forms. Then we find the possible configurations that give the scale-dependent bias.

As mentioned in section II, the general anisotropic power spectrum can be written as [47]

$$P(\vec{k}) = P_0(k) \left[1 + \sum_{LM} g_{LM}(k) Y_{LM}(\hat{k}) \right], \quad (57)$$

which is a generalization of our anisotropic power spectrum defined in Eq.(7), where all the k -dependence is buried in the coefficient g_{LM} . The anisotropic variance reads as:

$$\sigma_A^2(m, z) = \int d\psi d(\cos \theta) k^2 dk P_0(k, z) W(kR) \left[1 + \sum_{LM} g_{LM}(k) Y_{LM} \right]. \quad (58)$$

The spherical harmonics are orthonormal via

$$\int Y_{lm} Y_{l'm'}^* d\Omega = \delta_{ll'} \delta_{mm'}. \quad (59)$$

As a result, noting $Y_{00} = 1/\sqrt{4\pi}$, we have

$$\int Y_{lm} d\Omega = \sqrt{4\pi} \int Y_{lm} Y_{00}^* d\Omega = \sqrt{4\pi} \delta_{ll'} \delta_{mm'}, \quad (60)$$

so the variance, Eq.(58), can be simplified to

$$\sigma_A^2(m, z) = 4\pi \int k^2 dk P_0(k, z) W(kR) \left[1 + g_{00}(k)/\sqrt{4\pi} \right]. \quad (61)$$

Ignoring the scale-dependence of g_{00} , we have

$$\sigma_A^2(m, z) \simeq \sigma_0^2(m, z) \left[1 + g_{00}/\sqrt{4\pi} \right], \quad (62)$$

with

$$\sigma_0^2(m, z) = 4\pi \int k^2 dk P_0(k, z) W(kR). \quad (63)$$

Similarly, we can generalize the bispectrum in squeezed limit, where $k_3 \ll k_1 \approx k_2$, as follows

$$B_\zeta(\vec{k}_1, \vec{k}_2, \vec{k}_3) \approx 2 \sum_{L,l,m} c_{Llm} \mathcal{P}_L(\cos \theta_3) Y_{l,m}(\theta_1, \psi_1) \left(P_0(\vec{k}_1) P_0(\vec{k}_3) \right) \quad (64)$$

where \mathcal{P}_L is the Legendre function, $Y_{l,m}(\theta_1, \phi_1)$ are the spherical harmonics, by which the whole direction-dependence of bispectrum is encoded and the c_{Llm} are the k -dependent coefficients. This decomposition is possible because we set the z coordinate along the anisotropy direction and rotate the $x - y$ plane in Fourier (k -space) such that the azimuthal angle of k_3 is set to zero. We can do this rotation because of the symmetry in the $x - y$ plane. This kind of decomposition, i.e. decomposing into a k -dependent sector (c_{Llm}) and the angular-dependent part is especially useful to find the corresponding I_{21} term in the case of generic anisotropic bispectrum and the corresponding scale-dependent bias.

Since in the real space the bispectrum is a real quantity, and noting that the bispectrum above is defined in Fourier space, we find the condition

$$c_{Llm}^* = (-1)^{L+l} c_{Ll-m}. \quad (65)$$

Now, using Eq.(64), we can write I_{21} as

$$I_{21} = 2 \sum_{L,l,m} \int d\psi_1 d(\cos \theta_1) q^2 dq M_{m,z}(q) M_{m,z}(|k - q|) c_{Llm}(q, k) \mathcal{P}_L(\theta_3) Y_{l,m}(\theta_1, \psi_1) P_0(q), \quad (66)$$

which, again using the orthonormality of spherical harmonics, simplifies to

$$I_{21}(\mathbf{k}, m, z) = 4\sqrt{\pi} \sum_L \mathcal{P}_L(\cos \theta_k) \times \int q^2 dq M_{m,z}(q) M_{m,z}(|k - q|) c_{L,l=0,m=0}(q, k) P_0(q). \quad (67)$$

This is an interesting result showing that the anisotropic bispectrum induces an anisotropic, scale-dependent bias, through the Legendre function of the angle between the anisotropic direction \hat{n} and the long wavelength mode. It is also interesting to note that there is a *Selection Rule* for scale-dependent bias at $\mathcal{O}(f_{NL})$, where the harmonic numbers of the short wavelength must vanish ($l = 0, m = 0$). All the other parts of anisotropic bispectrum with $l, m \neq 0$, do not contribute to the leading order scale-dependent bias.

It is worth to mention that the reality assumption of the bispectrum implies

$$c_{L00}^* = (-1)^L c_{L00}, \quad (68)$$

where in the case of real c_{L00} we have to choose even L s. Now, if we define a direction-independent parameter $I_{(L)21}^{di}$ as

$$I_{(L)21}^{di}(k, m, z) \equiv 4\sqrt{\pi} \times \int q^2 dq M_{m,z}(q) M_{m,z}(|k - q|) c_{L00}(q, k) P_0(q), \quad (69)$$

then I_{21} will be re-expressed as

$$I_{21}(k, m, z, \theta_k) = \sum_L \mathcal{P}_L(\cos \theta_k) I_{(L)21}^{di}(k, m, z) \quad (70)$$

where θ_k is the angle between \hat{n} and \vec{k} . Now the scale-dependent bias becomes:

$$b_{2L}(k, z, m, \theta_k) = \frac{\sum_L \mathcal{P}_L(\cos \theta_k) I_{(L)21}^{di}(k, m, z)}{2\sigma_A^2(m, z)M(k, z)} \delta_c b_{1L} + \frac{1}{M(k, z)} \partial_{\ln \sigma_A^2} \left(\frac{\sum_L \mathcal{P}_L(\cos \gamma) I_{(L)21}^{di}(k, m, z)}{\sigma_A^2(m, z)} \right) \quad (71)$$

where in this case σ_A^2 is defined as in Eq.(61)

Our specific model of anisotropic inflation studied in previous Section corresponds to $L = 2, l = 0, m = 0$ with the corresponding coefficients.

VI. CONCLUSION AND DISCUSSIONS

The large scale structure observations, like the statistics of rare objects and the scale-dependence of bias parameter, can be used as complementary cosmological observations to CMB observations to constrain the inflationary models. In this work we obtained the scale and direction-dependent bias of dark matter halos in anisotropic inflationary models.

The anisotropic model used in this work has a bispectrum shape very close to the local non-Gaussianity shape with an extra mild k -dependence and also a direction-dependence. We showed that the bias parameter is mainly influenced by the angle (θ_{k_3}) between the anisotropy direction and the long wavelength mode k_3 in the squeezed limit by a factor $\sin^2 \theta_{k_3}$. An interesting observation is that the scale-dependent bias vanishes in linear order along the direction $\theta_{k_3} = 0, \pi$. This can be explained by the fact that the bispectrum vanishes in squeezed limit when the long wavelength mode is aligned to the anisotropy direction. This means that, at the level of bispectrum, the model reduces to the Gaussian model along this direction.

As it is clear from the PBS formalism, the bias parameter is mainly affected by the long wavelength mode. We can see this explicitly in our work where the angle between the anisotropy direction and the long mode appears in the bias formula.

The free parameter of our model is I . Recent CMB observations imply that $I \lesssim 10^{-5}$. Roughly speaking our bias parameter analysis also imply the same order of magnitude for I . Considering the fact that the observations are now in good agreement with a Gaussian bias we expect that in quasi-linear regime (where we have the strict constraint on bias) the ratio of $b_{sd}^{(A)}/b_G$ is at the order of one so from our results we also find $I \lesssim 10^{-5}$.

In this work we also formulated the general, model independent anisotropic scale dependent bias in linear order. For this purpose, by assuming rotational symmetry in $x - y$ plane of Fourier space, we modeled the bispectrum as a function of spherical harmonics, Y_{lm} / Logendre functions, \mathcal{P}_L , of the angles between the short/long wavelength modes and the anisotropic direction. Interestingly, we find a selection rule for scale-dependent anisotropic bias, which shows that the bias parameter only responses to the Y_{00} part of the anisotropic bispectrum. We also show that b_{sd} is independent of short wavelength mode and its direction. This is an obvious check for the formalism, since the bias should be only a function of the long wavelength mode.

In this work we assumed that the mechanism of spherical collapse and the conventional form of the transfer function are still applicable. This is motivated from the fact that the collapse of structures is a local mechanism which is less affected by the large scale anisotropies, although in principle it is an interesting question to see how one can generalize the spherical collapse mechanism in the presence of primordial anisotropic fluctuations. On the other hand, the modification of the transfer function due to Boltzmann and perturbed Einstein equations in the presence of a generic anisotropic cosmic fluid is an interesting question which is beyond the scope of this work.

Finally, it is an interesting open question to use the formalism we presented in this paper to compare more rigorously the predictions of models of anisotropic inflation to data from LSS observations to constrain the free parameters of these models.

Acknowledgments

We would like to thank Razieh Emami for many insightful discussions on anisotropic inflation.

Appendix A: Halos bias in the Peak Background Splitting in the context of Excursion Set Theory

In this appendix, first we review the Excursion Set theory (EST), then we will apply the Peak Background splitting (PBS) in EST context and finally we argue that how we can find the halo bias. In the context of Excursion Set theory (EST) halo formation can be described as the random walk of matter density contrast as the smoothing radius goes from very large radius, (corresponding to infinitesimal variance σ^2 , small δ) to the scales crossing the linear threshold for collapse δ_c at some finite smoothing radius. This radius is related to the scale in which the halos form. Within the EST formulation the number density of collapsed objects (dark matter halos of mass m) per unit mass is given by:

$$\left(\frac{dn}{dm}\right) = \frac{\bar{\rho}}{m} \partial_m \int_{-\infty}^{\delta_c} \Pi_0(\delta_s, \sigma_m^2, \delta_c) d\delta_s, \quad (\text{A1})$$

where σ_m^2 is the variance of the small scale density field smoothed with filter (window function) at spatial scale R and $\bar{\rho}$ is the background energy density, relating the halo mass to smoothing radius by $m = 4\pi\bar{\rho}R^3/3$. Furthermore, $\Pi_0(\delta_s, \sigma_m^2, \delta_c)$ is the unconditional probability distribution function (PDF) of small scale perturbations reaching δ_s (short wavelength density contrast) at variance σ^2 . By the subscript 0 as well as the *unconditional* for PDF, we mean that the initial condition (first step in random walk) is $\delta_s = 0$ where $\sigma_m^2 = 0$, and it satisfies the absorbing barrier condition $\Pi_0(\delta_c, \sigma_m^2, \delta_c) = 0$.

The smoothing procedure will be done by top-hat window function [68]

$$W(x) = \frac{3(\sin x - x \cos x)}{x^3}. \quad (\text{A2})$$

The lagrangian radius of collapsed objects is related to the mass via:

$$R = \left[\frac{m}{1.162 \times 10^{12} h^2 M_\odot \Omega_m^0} \right]^{1/3} \text{Mpc} \quad (\text{A3})$$

where m is the mass of the structure and $\Omega_m = \Omega_m^0(1+z)^3$.

In the Extended Press-Schechter (EPS) formalism the variance σ_m is a monotonic function of mass scale so we use it as the clock. So it will be relevant to define a quantity that shows the probability of first up-crossing in the time σ_m^2 and $\sigma_m^2 + d\sigma_m^2$ as:

$$\mathcal{F}_0(\delta_c, \sigma_m^2) \equiv -\frac{\partial}{\partial \sigma_m^2} \int_{-\infty}^{\delta_c} \Pi_0(\delta_s, \sigma_m^2, \delta_c) d\delta_s, \quad (\text{A4})$$

Now the number density of collapsed objects will be:

$$\left(\frac{dn}{dm}\right) = \frac{\bar{\rho}}{m} \left| \frac{d\sigma_m^2}{dm} \right| \times \mathcal{F}_0(\delta_c, \sigma_m^2), \quad (\text{A5})$$

It is worth to mention that the number density of dark matter halos obeys the normalization condition:

$$\int \left(\frac{dn}{dm}\right) m dm = \bar{\rho} \quad (\text{A6})$$

An important parameter in mass function of structures is the density contrast power spectrum, defined by [68]

$$P_L(k) = A k^{n_s} T^2(k) D^2(z), \quad (\text{A7})$$

where n_s is the spectral index, A is the linear matter primordial power spectrum amplitude in $k = 0.002 h^{-1} \text{Mpc}$, $T(k)$ the transfer function, and $D(z)$ is the growth factor normalized to scale factor at early times.

The evolution of density contrast is imprinted in growth function $D(z)$ and the transfer function $T(k)$, showing the scale-dependence of gravitational potential during cosmic evolution. In this work we use the growth function of standard ΛCDM cosmology and the transfer function of Bardeen, Bond, Kaiser and Szalay (BBKS) [57] respectively as below:

$$D(z) = \frac{5}{2} \frac{1}{1+z} \Omega_m \left[\Omega_m^{4/7} - \Omega_\Lambda + \left(1 + \frac{\Omega_m}{2}\right) \left(1 + \frac{\Omega_\Lambda}{70}\right) \right]^{-1}, \quad (\text{A8})$$

and

$$T(k = q\Omega_m h^2 Mpc^{-1}) \approx \frac{\ln[1 + 2.34q]}{2.34q} \times [1 + 3.89q + (16.2q)^2 + (5.47q)^3 + (6.71q)^4]^{-1/4}. \quad (A9)$$

A crucial point to indicate is that the variance has a linear dependence to growth function $\sigma^2(M, z) = \sigma^2(M)D^2(z)$, where $\sigma^2(M)$ is the present value of variance. This redshift-dependance is important in the sense that the statistics of structure and even the bias parameter will be redshift-dependent. In upcoming section we will show the redshift-dependence of bias parameter. In the matter dominated era $D(z)$ scales like $1/(1+z)$ which is a decreasing function with respect to redshift. Now that we set the matter density variance and large scale statistics of matter distribution, by setting the initial condition of perturbations we can find the mass function of structures in the Universe. For the Gaussian initial condition the probability distribution function (PDF) in Fourier-space top-hat filter is:

$$\Pi_0(\delta_s, \sigma_m^2, \delta_c) = \mathcal{P}_G(\delta_s, \sigma_m^2) - \mathcal{P}_G(2\delta_c - \delta_s, \sigma_m^2), \quad (A10)$$

where \mathcal{P}_G is the Gaussian PDF.

The assumption of the universality of mass-function (i.e. Press-Schechter) yields

$$\Pi_0(\delta_s, \sigma_m^2, \delta_c) = F\left(\frac{\delta_s}{\sigma_m}, \frac{\delta_c}{\sigma_m}\right), \quad (A11)$$

which leads us to write $\sigma_m^2 \mathcal{F}_0$ just as a function of threshold quantity $\nu = \delta_c/\sigma_m$:

$$\sigma_m^2 \mathcal{F}_0(\delta_c, \sigma_m^2) = \frac{\nu f(\nu)}{2}, \quad (A12)$$

where $f(\nu)$ is the usual Gaussian factor in Press-Schechter theory[17]. Now in order to find the halo bias term in Gaussian and non-Gaussian inflationary models, first we discuss the PBS. We will show how this method is applicable for non-Gaussian fields.

For inflationary models with primordial non-Gaussianity, the gravitational potential is usually written as [69–71]

$$\Phi(x) = \phi(x) + f_{NL}([\phi(x)]^2 - \langle \phi^2 \rangle) \quad (A13)$$

where ϕ is a Gaussian random field. The above relation is the simplest extension of Bardeen potential to include non-linearity, called local non-Gaussianity. We can generalize the local type non-Gaussianity to arbitrary shape, simply by replacing the non-linear term by a kernel [48]

$$\Phi(x) = \phi(x) + f_{NL}K[\phi(x), \phi(x)]. \quad (A14)$$

In order to obtain the bias parameter, we can use the Peak-Background Splitting idea on the Gaussian potential $\phi = \phi_s + \phi_l$, where ϕ_l is the long-wavelength mode of the potential and ϕ_s is the short-wavelength mode. Since the large scale perturbations change the background for small scale modes, the PDF of small scale perturbations is modified to conditional PDF, $\Pi(\delta_s, \sigma_m^2, \delta_c; \delta_l, \sigma_l^2)$. In conditional PDF, the initial condition is $\sigma_m \rightarrow \sigma_l$ in large scale limit (first step in random walk), in contrast with the unconditional case in which the variance vanishes on large scales.

On the other hand, the existence of any type of non-Gaussianity modifies the PDF such that it is no longer independent of higher cumulants, while in Gaussian case the PDF is completely determined by zeroth (δ_s) and first (σ_m^2) order cumulants.

By the splitting procedure explained above, and noting that the PDF is now a function of all cumulants, we can expand the Lagrangian halo overdensity as an expansion over large-scale ϕ modes [48],

$$\delta_h^L = \int d^3k \frac{\partial_m \int_{-\infty}^{\delta_c} d\delta_s (D\Pi/D\phi_l)_0}{\partial_m \int_{-\infty}^{\delta_c} d\delta_s \Pi_0(\delta_s, \sigma^2, \delta_c)} \phi_l + \frac{1}{2} \int \int d^3k_1 d^3k_2 \frac{\partial_m \int_{-\infty}^{\delta_c} d\delta_s (D^2\Pi/D\phi_l D\phi_l)_0}{\partial_m \int_{-\infty}^{\delta_c} d\delta_s \Pi_0(\delta_s, \sigma^2, \delta_c)} \times \phi_l(\vec{k}_1) \phi_l(\vec{k}_2) + \dots \quad (A15)$$

where $(\dots)_0$ means that the corresponding quantity is evaluated at $\phi_l = 0$. Note that because the background is now modified by large scale perturbation ϕ_l , the cumulants are now functions of ϕ_l . The first derivative in Eq.(A15), to all orders in primordial non-Gaussianity, is

$$\left(\frac{D\Pi}{D\phi_l(\vec{k})}\right)_0 = \sum_{p=1}^{\infty} \left(\frac{\partial \Pi}{\partial c^{(p)}}\right)_0 \left(\frac{Dc^{(p)}}{D\phi_l(\vec{k})}\right)_0 = \left(\frac{\partial \Pi}{\partial \delta_l}\right)_0 \left(\frac{D\delta_l}{D\phi_l(\vec{k})}\right) + \sum_{p=2}^{\infty} \frac{\partial \Pi_0}{\partial c_m^{(p)}} \left(\frac{Dc^{(p)}}{D\phi_l(\vec{k})}\right)_0 \quad (A16)$$

where the cumulants are defined by

$$c^{(1)} \equiv \delta_l, \quad c_m^{(2)} \equiv \sigma_m^2, \quad c^{(2)} \equiv \sigma^2(\phi_l), \quad c_m^{(p)} \equiv \langle \delta_s^p \rangle_c, \quad c^{(p)} \equiv \langle \delta_s^p(\phi_l) \rangle_c \quad (\text{A17})$$

in which the subscript m for cumulants show that they are evaluated without the background ϕ_l (independent of ϕ_l). It is worth to indicate that to first order in f_{NL} , only the first two terms in the Taylor expansion above ($p = 1, 2$) contributes to the bias, while $p = 3$ contributes to $\mathcal{O}(f_{NL}^2)$ and $\mathcal{O}(g_{NL})$.

Now we can obtain the bias parameter, using the above formulation. The $p = 1$ contribution is the usual scale-independent bias presented in initially Gaussian case. Keeping in mind $b \equiv \delta_h/\delta_l$, we have

$$p = 1: \quad b_{1L} = \frac{\partial_m \int (\partial \Pi / \partial \delta_l)_0}{\partial_m \int \Pi_0} = \left[\frac{\partial}{\partial \delta_l} \ln \left(\frac{dn(\delta_l)}{d \ln m} \right) \right], \quad (\text{A18})$$

which can be simplified as

$$b_{1L} = \frac{\partial}{\partial \delta_l} \ln(n(\delta_l)) \quad (\text{A19})$$

The $p = 2$ contribution is the scale-dependent correction to the leading order bias coming from primordial non-Gaussianity

$$p = 2: \quad b_{2L} = \frac{\partial_m [I_{21} \int \partial \Pi_0 / \partial \sigma_m^2]}{M(k) \partial_m \int \Pi_0} \quad (\text{A20})$$

The quantity I_{21} includes the information about the primordial non-Gaussianity, and it is the derivative of second cumulant σ_m^2 , ($p=2$), with respect to long wavelength mode ϕ_l which is obtained as [48]:

$$I_{21}(k, m) = \frac{1}{P_\phi(k)} \int B_{\hat{\delta}\hat{\delta}\phi}(q, k - q, -k) d^3 q, \quad (\text{A21})$$

where $B_{\hat{\delta}\hat{\delta}\phi}$ is cross bispectrum of small-scale smoothed density $\hat{\delta}$ and ϕ .

So far the Lagrangian bias appeared, because peaks are those of the initial density field (linearly extrapolated). By the standard assumptions that halos move coherently with the underlying dark matter, one can obtain the final Eulerian bias as:

$$b_E = 1 + b_{1L} + b_{2L}, \quad (\text{A22})$$

using the techniques outlined in [60–63].

Note that, due to the existence of primordial non-Gaussianity, the leading order scale-independent bias also modifies. Assuming the Markovian behavior of density fields and universality of mass function we have

$$b_{1L} = \frac{2}{\delta_c} \partial_{\ln \sigma_m^2} \ln(\sigma_m^2 \mathcal{F}) = b_{1L(G)} + b_{1L(NG)}, \quad (\text{A23})$$

where in the Eq.(A23) we omit the subscript of \mathcal{F} , which means that the Non-Gaussianity will change the PDF of structures, resulting in a modification of b_{1L} . As a result we have:

$$b_{1L(G)} = \frac{2}{\delta_c} \partial_{\ln \sigma_m^2} \ln(\sigma_m^2 \mathcal{F}_0) \quad (\text{A24})$$

and

$$b_{1L(NG)} = \frac{2}{\delta_c} \partial_{\ln \sigma_m^2} \ln(\sigma_m^2 \mathcal{R}_{NG}) = \frac{\partial \ln \mathcal{R}_{NG}(m, f_{NL})}{\partial \delta_l}, \quad (\text{A25})$$

as described in Section (III).

$$\mathcal{R}_{NG}(m, f_{NL}) = 1 + \frac{1}{6} x(x^2 - 3) s_3(x) - \frac{1}{6} (x - 1/x) \frac{ds_3(x)}{d \ln(x)}, \quad (\text{A26})$$

where $x \equiv \delta_c/\sigma_M$, $\delta_c = 1.68$ is the critical density and s_3 is the reduced skewness defined as:

$$s_3(R) \equiv \frac{\langle \delta_R^3 \rangle}{\langle \delta_R^2 \rangle^{3/2}} = \frac{\langle \delta_R^3 \rangle}{\sigma_m^3}, \quad (\text{A27})$$

The skewness is related to the matter bispectrum as:

$$\langle \delta_R^3 \rangle = \int \frac{d^3 q_1}{(2\pi)^3} \frac{d^3 q_2}{(2\pi)^3} W(Rq_1) W(Rq_2) W(Rq_{12}) M(q_1, z) M(q_2, z) M(q_{12}, z) B_0(q_1, q_2, q_{12}), \quad (\text{A28})$$

where $q_{12} = q_1 + q_2$ and $W(kR)$ is the window function in Fourier space, smoothing perturbations up to scale R .

In obtaining the PDF of non-Gaussianity model in this approximation, we have assumed that all the deviation is imprinted in the skewness which may not be entirely true. In order to improve the results, numerical simulations are done [22, 72, 73]. Consequently, a scaling parameter κ defined by $R_{NG}(x) \rightarrow R_{NG}(\kappa x)$ are introduced where, in the work of [74], from simulation of [75], it is obtained to be $\kappa = 0.91$. (For a similar correction from simulation you can see [76])

On the other hand, the scale-dependent bias can be rewritten by

$$b_{2L} = \frac{I_{21}(k, m)}{2\sigma_m^2 M(k, z)} \delta_c b_{1L} + \frac{1}{M(k, z)} \partial_{\ln \sigma_m^2} \left(\frac{I_{21}(k, m)}{\sigma_m^2} \right) \quad (\text{A29})$$

So the total Eulerian bias up to first order in f_{NL} can be splitted to scale-independent b_{si} and scale-dependent b_{sd} terms as:

$$b_t = b_{si} + b_{sd} \quad (\text{A30})$$

where b_{si} and b_{sd} are:

$$b_{si} \equiv b_G + b_{1L(NG)}, \quad (\text{A31})$$

with $b_G \equiv 1 + b_{1L(G)}$ and

$$b_{sd} = b_{2L} + \mathcal{O}(f_{NL}^2) + \mathcal{O}(g_{NL}) + \dots \quad (\text{A32})$$

-
- [1] A. H. Guth, “The Inflationary Universe: A Possible Solution To The Horizon And Flatness Problems,” *Phys. Rev. D* **23**, 347 (1981);
 K. Sato, “First Order Phase Transition of a Vacuum and Expansion of the Universe,” *Mon. Not. Roy. Astron. Soc.* **195**, 467-479 (1981).
 A. D. Linde, “A New Inflationary Universe Scenario: A Possible Solution Of The Horizon, Flatness, Homogeneity, Isotropy And Primordial Monopole Problems,” *Phys. Lett. B* **108**, 389 (1982);
 A. Albrecht and P. J. Steinhardt, “Cosmology For Grand Unified Theories With Radiatively Induced Symmetry Breaking,” *Phys. Rev. Lett.* **48**, 1220 (1982).
- [2] G. Hinshaw, D. Larson, E. Komatsu, D. N. Spergel, C. L. Bennett, J. Dunkley, M. R. Nolta and M. Halpern *et al.*, “Nine-Year Wilkinson Microwave Anisotropy Probe (WMAP) Observations: Cosmological Parameter Results,” arXiv:1212.5226 [astro-ph.CO].
- [3] X. Chen, “Primordial Non-Gaussianities from Inflation Models,” *Adv. Astron.* **2010**, 638979 (2010) [arXiv:1002.1416 [astro-ph.CO]].
- [4] E. Komatsu, “Hunting for Primordial Non-Gaussianity in the Cosmic Microwave Background,” *Class. Quant. Grav.* **27**, 124010 (2010) [arXiv:1003.6097 [astro-ph.CO]].
- [5] N. Bartolo, S. Matarrese and A. Riotto, “Non-Gaussianity and the Cosmic Microwave Background Anisotropies,” *Adv. Astron.* **2010**, 157079 (2010) [arXiv:1001.3957 [astro-ph.CO]].
- [6] J. M. Maldacena, “Non-Gaussian features of primordial fluctuations in single field inflationary models,” *JHEP* **0305**, 013 (2003) [astro-ph/0210603].
- [7] M. H. Namjoo, H. Firouzjahi and M. Sasaki, “Violation of non-Gaussianity consistency relation in a single field inflationary model,” arXiv:1210.3692 [astro-ph.CO].
- [8] X. Chen, H. Firouzjahi, M. H. Namjoo and M. Sasaki, “A Single Field Inflation Model with Large Local Non-Gaussianity,” arXiv:1301.5699 [hep-th].

- [9] I. Agullo and L. Parker, “Non-gaussianities and the Stimulated creation of quanta in the inflationary universe,” *Phys. Rev. D* **83**, 063526 (2011) [arXiv:1010.5766 [astro-ph.CO]].
- [10] J. Ganc, “Calculating the local-type fNL for slow-roll inflation with a non-vacuum initial state,” *Phys. Rev. D* **84**, 063514 (2011) [arXiv:1104.0244 [astro-ph.CO]].
- [11] D. Chialva, “Signatures of very high energy physics in the squeezed limit of the bispectrum (violation of Maldacena’s condition),” *JCAP* **1210**, 037 (2012).
- [12] E. Komatsu, B. D. Wandelt, D. N. Spergel, A. J. Banday and K. M. Gorski, “Measurement of the cosmic microwave background bispectrum on the COBE DMR sky maps,” *Astrophys. J.* **566**, 19 (2002) [astro-ph/0107605].
- [13] E. Komatsu, D. N. Spergel and B. D. Wandelt, “Measuring primordial non-Gaussianity in the cosmic microwave background,” *Astrophys. J.* **634**, 14 (2005) [astro-ph/0305189].
- [14] N. Dalal, O. Dore, D. Huterer and A. Shirokov, “The imprints of primordial non-gaussianities on large-scale structure: scale dependent bias and abundance of virialized objects,” *Phys. Rev. D* **77**, 123514 (2008) [arXiv:0710.4560 [astro-ph]].
- [15] R. Scoccimarro, E. Sefusatti and M. Zaldarriaga, “Probing primordial non-Gaussianity with large - scale structure,” *Phys. Rev. D* **69**, 103513 (2004) [astro-ph/0312286].
- [16] V. Desjacques and U. Seljak, “Primordial non-Gaussianity in the large scale structure of the Universe,” *Adv. Astron.* **2010**, 908640 (2010) [arXiv:1006.4763 [astro-ph.CO]].
- [17] W. H. Press and P. Schechter, “Formation of galaxies and clusters of galaxies by selfsimilar gravitational condensation,” *Astrophys. J.* **187**, 425 (1974).
- [18] L. Verde, “Non-Gaussianity from Large-Scale Structure Surveys,” *Adv. Astron.* **2010**, 768675 (2010) [arXiv:1001.5217 [astro-ph.CO]].
- [19] S. Matarrese, L. Verde and R. Jimenez, “The Abundance of high-redshift objects as a probe of non-Gaussian initial conditions,” *Astrophys. J.* **541**, 10 (2000) [astro-ph/0001366].
- [20] M. Kamionkowski, L. Verde and R. Jimenez, “The Void Abundance with Non-Gaussian Primordial Perturbations,” *JCAP* **0901**, 010 (2009) [arXiv:0809.0506 [astro-ph]].
- [21] M. LoVerde, A. Miller, S. Shandera and L. Verde, “Effects of Scale-Dependent Non-Gaussianity on Cosmological Structures,” *JCAP* **0804**, 014 (2008) [arXiv:0711.4126 [astro-ph]].
- [22] M. Grossi, L. Verde, C. Carbone, K. Dolag, E. Branchini, F. Iannuzzi, S. Matarrese and L. Moscardini, “Large-scale non-Gaussian mass function and halo bias: tests on N-body simulations,” *Mon. Not. Roy. Astron. Soc.* **398**, 321 (2009) [arXiv:0902.2013 [astro-ph.CO]].
- [23] P. Catelan, F. Lucchin, S. Matarrese, and L. Moscardini. Eulerian perturbation theory in non-flat universes: second-order approximation. *MNRAS*, 276:3956, September 1995.
- [24] S. Matarrese and L. Verde, “The effect of primordial non-Gaussianity on halo bias,” *Astrophys. J.* **677**, L77 (2008) [arXiv:0801.4826 [astro-ph]].
- [25] T. Giannantonio, A. J. Ross, W. J. Percival, R. Crittenden, D. Bacher, M. Kilbinger, R. Nichol and J. Weller, arXiv:1303.1349 [astro-ph.CO].
- [26] T. G. Sarkar and D. K. Hazra, arXiv:1211.4756 [astro-ph.CO].
- [27] D. K. Hazra and T. G. Sarkar, “Primordial Non-Gaussianity in the Forest: 3D Bispectrum of Ly-alpha Flux Spectra Along Multiple Lines of Sight,” *Phys. Rev. Lett.* **109**, 149902 (2012) [arXiv:1205.2790 [astro-ph.CO]].
- [28] G. D’Amico, M. Musso, J. Norena and A. Paranjape, “Excursion Sets and Non-Gaussian Void Statistics,” *Phys. Rev. D* **83**, 023521 (2011) [arXiv:1011.1229 [astro-ph.CO]].
- [29] D. Hanson, A. Lewis, “Estimators for CMB Statistical Anisotropy,” *Phys. Rev. D* **80**, 063004 (2009). [arXiv:0908.0963 [astro-ph.CO]].
- [30] D. Hanson, A. Lewis, A. Challinor, “Asymmetric Beams and CMB Statistical Anisotropy,” *Phys. Rev. D* **81**, 103003 (2010). [arXiv:1003.0198 [astro-ph.CO]].
- [31] L. Ackerman, S. M. Carroll and M. B. Wise, “Imprints of a Primordial Preferred Direction on the Microwave Background,” *Phys. Rev. D* **75**, 083502 (2007) [Erratum-ibid. *D* **80**, 069901 (2009)] [astro-ph/0701357].
- [32] N. E. Groeneboom, L. Ackerman, I. K. Wehus and H. K. Eriksen, “Bayesian analysis of an anisotropic universe model: systematics and polarization,” *Astrophys. J.* **722**, 452 (2010) [arXiv:0911.0150 [astro-ph.CO]].
- [33] A. R. Pullen and C. M. Hirata, “Non-detection of a statistically anisotropic power spectrum in large-scale structure,” *JCAP* **1005**, 027 (2010) [arXiv:1003.0673 [astro-ph.CO]].
- [34] M. a. Watanabe, S. Kanno and J. Soda, “Inflationary Universe with Anisotropic Hair,” *Phys. Rev. Lett.* **102**, 191302 (2009) [arXiv:0902.2833 [hep-th]].
- [35] N. Bartolo, S. Matarrese, M. Peloso and A. Ricciardone, “The anisotropic power spectrum and bispectrum in the $f(\phi)F^2$ mechanism,” arXiv:1210.3257 [astro-ph.CO].
- [36] M. Shiraishi, E. Komatsu, M. Peloso and N. Barnaby, “Signatures of anisotropic sources in the squeezed-limit bispectrum of the cosmic microwave background,” arXiv:1302.3056 [astro-ph.CO].
- [37] A. A. Abolhasani, R. Emami, J. T. Firouzjaee and H. Firouzjahi, “ δN Formalism in Anisotropic Inflation and Large Anisotropic Bispectrum and Trispectrum,” arXiv:1302.6986 [astro-ph.CO].
- [38] D. H. Lyth and M. Karčiauskas, “The statistically anisotropic curvature perturbation generated by $f(\phi)^2 F^2$,” arXiv:1302.7304 [astro-ph.CO].
- [39] M. S. Turner and L. M. Widrow, “Inflation Produced, Large Scale Magnetic Fields,” *Phys. Rev. D* **37**, 2743 (1988).
- [40] B. Ratra, “Cosmological ‘seed’ magnetic field from inflation,” *Astrophys. J.* **391**, L1 (1992).
- [41] K. Yamamoto, “Primordial Fluctuations from Inflation with a Triad of Background Gauge Fields,” *Phys. Rev. D* **85**, 123504 (2012) [arXiv:1203.1071 [astro-ph.CO]].

- [42] R. Emami and H. Firouzjahi, “Curvature Perturbations in Anisotropic Inflation with Symmetry Breaking,” arXiv:1301.1219 [hep-th].
- [43] T. R. Dulaney, M. I. Gresham, “Primordial Power Spectra from Anisotropic Inflation,” Phys. Rev. **D81**, 103532 (2010). [arXiv:1001.2301 [astro-ph.CO]].
- [44] A. E. Gumrukcuoglu, B. Himmetoglu, M. Peloso, “Scalar-Scalar, Scalar-Tensor, and Tensor-Tensor Correlators from Anisotropic Inflation,” Phys. Rev. **D81**, 063528 (2010). [arXiv:1001.4088 [astro-ph.CO]].
- [45] M. a. Watanabe, S. Kanno and J. Soda, “The Nature of Primordial Fluctuations from Anisotropic Inflation,” Prog. Theor. Phys. **123**, 1041 (2010) [arXiv:1003.0056 [astro-ph.CO]].
- [46] H. Funakoshi and K. Yamamoto, “Primordial bispectrum from inflation with background gauge fields,” arXiv:1212.2615 [astro-ph.CO].
- [47] A. R. Pullen and M. Kamionkowski, “Cosmic Microwave Background Statistics for a Direction-Dependent Primordial Power Spectrum,” Phys. Rev. D **76**, 103529 (2007) [arXiv:0709.1144 [astro-ph]].
- [48] R. Scoccimarro, L. Hui, M. Manera and K. C. Chan, “Large-scale Bias and Efficient Generation of Initial Conditions for Non-Local Primordial Non-Gaussianity,” Phys. Rev. D **85**, 083002 (2012) [arXiv:1108.5512 [astro-ph.CO]].
- [49] J.R. Bond, S. Cole, G. Efstathiou and N. Kaiser, Astrophys. J. **379**, 440 (1991).
- [50] R. K. Sheth and G. Lemson, [astro-ph/9808138].
- [51] H. J. Mo, Y. P. Jing and S. D. M. White, “High-order correlations of peaks and halos: A Step toward understanding galaxy biasing,” astro-ph/9603039.
- [52] R. Scoccimarro, R. K. Sheth, L. Hui and B. Jain, “How many galaxies fit in a halo? Constraints on galaxy formation efficiency from spatial clustering,” Astrophys. J. **546**, 20 (2001) [astro-ph/0006319].
- [53] R. E. Smith, R. Scoccimarro and R. K. Sheth, Phys. Rev. D **75**, 063512 (2007) [astro-ph/0609547].
- [54] M. Manera, R. KSheth and R. Scoccimarro, arXiv:0906.1314 [astro-ph.CO].
- [55] M. Manera and E. Gaztanaga, arXiv:0912.0446 [astro-ph.CO].
- [56] S. Cole and N. Kaiser, Mon. Not. R. Astron. Soc. **237**, 1127 (1989)
- [57] J. M. Bardeen, J. R. Bond, N. Kaiser and A. S. Szalay, “The Statistics of Peaks of Gaussian Random Fields,” Astrophys. J. **304**, 15 (1986).
- [58] J. E. Gunn and J. R. Gott, III, “On the Infall of Matter into Clusters of Galaxies and Some Effects on Their Evolution,” Astrophys. J. **176**, 1 (1972).
- [59] A. Slosar, C. Hirata, U. Seljak, S. Ho and N. Padmanabhan, JCAP **68**, 031 (2008).
- [60] H. J. Mo and S. D. M. White, “An Analytic model for the spatial clustering of dark matter halos,” Mon. Not. Roy. Astron. Soc. **282**, 347 (1996) [astro-ph/9512127].
- [61] P. Catelan, F. Lucchin, S. Matarrese and C. Porciani, “The bias field of dark matter halos,” Mon. Not. Roy. Astron. Soc. **297**, 692 (1998) [astro-ph/9708067].
- [62] G. Efstathiou, C. S. Frenk, S. D. M. White and M. Davis, “Gravitational clustering from scale free initial conditions,” Mon. Not. Roy. Astron. Soc. **235**, 715 (1988).
- [63] S. Cole and N. Kaiser, Mon. Not. Roy. Astron. Soc. **237**, 1127 (1989).
- [64] E. Sefusatti, C. Vale, K. Kadota and J. Frieman, “Primordial non-Gaussianity and Dark Energy constraints from Cluster Surveys,” Astrophys. J. **658**, 669 (2007) [astro-ph/0609124].
- [65] R. K. Sheth and G. Tormen, “Large scale bias and the peak background split,” Mon. Not. Roy. Astron. Soc. **308**, 119 (1999) [astro-ph/9901122].
- [66] M. Shiraishi, S. Yokoyama, K. Ichiki and T. Matsubara, “Scale-dependent bias due to primordial vector field,” arXiv:1301.2778 [astro-ph.CO].
- [67] E. Sefusatti, J. R. Fergusson, X. Chen and E. P. S. Shellard, “Effects and Detectability of Quasi-Single Field Inflation in the Large-Scale Structure and Cosmic Microwave Background,” JCAP **1208**, 033 (2012) [arXiv:1204.6318 [astro-ph.CO]].
- [68] S. Weinberg, *Cosmology*, Oxford University Press, (2008).
- [69] D.S. Salopek and J.R. Bond, Phys. Rev. D **43**, 1005 (1991).
- [70] D. S. Salopek and J. R. Bond, “Nonlinear evolution of long wavelength metric fluctuations in inflationary models,” Phys. Rev. D **42** (1990) 3936.
- [71] E. Komatsu and D. N. Spergel, “Acoustic signatures in the primary microwave background bispectrum,” Phys. Rev. D **63**, 063002 (2001) [astro-ph/0005036].
- [72] M. Maggiore and A. Riotto, “The Halo mass function from excursion set theory. III. Non-Gaussian fluctuations,” Astrophys. J. **717**, 526 (2010) [arXiv:0903.1251 [astro-ph.CO]].
- [73] A. Paranjape, C. Gordon and S. Hotchkiss, “The Extreme Tail of the Non-Gaussian Mass Function,” Phys. Rev. D **84**, 023517 (2011) [arXiv:1104.1145 [astro-ph.CO]].
- [74] E. Sefusatti, M. Crocce and V. Desjacques, “The Halo Bispectrum in N-body Simulations with non-Gaussian Initial Conditions,” arXiv:1111.6966 [astro-ph.CO].
- [75] V. Desjacques, U. Seljak and I. Iliev, “Scale-dependent bias induced by local non-Gaussianity: A comparison to N-body simulations,” arXiv:0811.2748 [astro-ph].
- [76] J. L. Tinker, A. V. Kravtsov, A. Klypin, K. Abazajian, M. S. Warren, G. Yepes, S. Gottlober and D. E. Holz, Astrophys. J. **688**, 709 (2008) [arXiv:0803.2706 [astro-ph]].